Pergamon

0031-9422(95)00170-O

Phytochemistry, Vol. 39, No. 5, pp. 959–968, 1995

0031-9422/95 $9.50 + 0.00

UV-INDUCED CROSS-LINKING OF ABSCISIC ACID TO BINDING PROTEINS

MATHIJS H. M. CORNELUSSEN,* CEES M. KARSSEN and LEENDERT C. VAN LOON†

Department of Plant Physiology, Agricultural University Wageningen, Arboretumlaan 4, NL-6703 BD Wageningen, The Netherlands

(*Received in revised form* 6 *December* 1994)

Key Word Index—Photoaffinity labelling; abscisic acid; abscisic acid-binding protein; enzyme immunoassay; mouse antibody.

Abstract—Conditions for UV-induced cross-linking of abscisic acid (ABA) through its enone chromophore to binding proteins were evaluated. The effects of a UV-light band between 260 and 530 nm on both unconjugated and protein-conjugated ABA, as well as on anti-ABA antibodies as models of ABA-binding proteins were determined. UV irradiation caused both isomerization and photolysis of ABA, but increasing the lower irradiation boundary to 345 nm strongly reduced photolysis and largely prevented isomerization. When conjugated to alkaline phosphatase (AP), ABA remained stable when using either a 320 or a 345 nm filter. At these wavelengths both binding of ABA to antibodies as well as AP enzymatic activity were maintained. UV-induced cross-linking of monoclonal anti-ABA antibodies to immobilized ABA was analysed by immunoassays. Optimal cross-linking was achieved after a 5 min irradiation period at 0°, using a long pass, cut-on filter to quench wavelengths below 290 nm. This cross-linking faithfully reflected cognate binding activity.

INTRODUCTION

It is commonly assumed that plant hormones regulate developmental processes in plants through their interaction with one or more hormone-binding proteins. Owing to their low abundance relative to other proteins, binding proteins are difficult to identify, requiring the use of advanced biochemical techniques [1].

In 1984 Hornberg and Weiler [2] reported the occurrence of specific ABA-binding proteins on the plasmalemma of guard-cell protoplasts. They were able to label these proteins by UV-induced covalent attachment of ABA. Contrary to other photoaffinity labels used to identify receptors for other plant hormones, the ABA molecule was not modified (see refs cited in [3]). However, the ABA-binding protein(s) were not characterized. Surprisingly, UV cross-linking of unmodified ABA to target proteins does not seem to have been investigated further. Instead, azido-C_1-ABA was introduced as an alternative photoaffinity label [4]. Yet, both azido-ABA and unmodified ABA contain a UV-sensitive, α,β-unsaturated ketone moiety (an enone structure) in their rings.

Enone-containing ligands have been successfully used in photoaffinity labelling [5–7]. Although this technique proved its potential in identifying specific binding proteins and evaluation of target sites on enzymes [5–8], it also imposes strict requirements (Table 1). Conditions have to be optimized to ensure that non-specific labelling is avoided and radiation damage to both binding protein and ligand is minimal, while maximal cross-linking efficiency is maintained.

Unmodified ABA meets these demands for a photoaffinity ligand. Contrary to azido- and diazo-compounds, the lifetimes of excited intermediates derived from enone are not known to exceed 100 μsec [6]. Excitation of enones can occur in two ways: a $\pi \rightarrow \pi^*$ transition or a $n \rightarrow \pi^*$ transition [9]. Both transitions result in an intermediate possessing a diradical-like character [5, 7, 9], but only the $n \rightarrow \pi^*$ transition will lead to cross-linking [5, 6, 9]. The $\pi \rightarrow \pi^*$ transition will mainly lead to undesirable side-effects, such as skeletal rearrangements [9], photo-oxidation [10], inactivation without cross-linking [5, 10] and amino acid/protein photolysis [11].

Apart from specific affinity labelling, UV-induced cross-linking can also lead to pseudo-affinity labelling and to non-specific attachment [5, 12–14] due to the excitation of non-bound molecules. To minimize these undesirable side-effects complete separation of these non-bound from bound ligands is imperative. This can be achieved by centrifugation [2], gel filtration/charcoal absorption [7] or ammonium sulphate precipitation [15] (although this latter is not recommended [16]). However,

*Supported by the Netherlands Organisation for Scientific Research—Foundation for Life Sciences (NWO-SLW) under grant number 805.21.901.

†Present address: Department of Plant Ecology and Evolutionary Biology, Utrecht University, Post Office Box 80084, NL-3508 TB Utrecht, The Netherlands.

Table 1. Requirements for photo-affinity labelling. Adapted from refs [5, 7, 28]

Photoaffinity ligand	• Biologically active in either inducing or blocking physiological response[a] • Stable in storage and handling prior to irradiation • Easily labelled and/or synthesized • Short-lived excited intermediates
Ligand–macromolecule complex	• Specific complex formation • Dissociation negligible during experiment • Stable cross-linked complexes • Ready separation of cross-linked and non-cross-linked complexes
Conditions	• Minimal damage to macromolecule and ligand • No free ligand present in solution • Minimal photo-oxidation • Inclusion of nucleophiles to reduce free radicals

[a]The photoaffinity ligand is assumed to interact at the same binding site as the natural ligand. This is difficult to prove in bioassays: the photoaffinity ligand may use a different route to induce or to inhibit a physiological response. Binding studies can only be used to verify the competition between the two ligands in cell-free extracts, provided labelling does not fall below the assay's detection level.

separation can be greatly facilitated when either binding protein or photosensitive ligand is immobilized on a matrix.

ABA can be conjugated through its carboxylic acid moiety to primary amines [17] leaving the enone structure exposed for photoaffinity cross-linking. Coating microtitre plates with an ABA-C_1-carrier protein conjugate effectively offers an immobilized photoactive ligand to a binding protein in solution. Proteins interacting with ABA through the unmodified ring structure will be cross-linked upon UV irradiation. Since monoclonal anti-ABA antibodies can be traced by immunological techniques, they can serve as specific and easily detectable model ABA-binding proteins. Thus, the effects of UV irradiation on both ABA and protein stability, as well as on photoinduced cross-linking, can be determined in order to optimize this technique for subsequent identification of ABA-binding proteins in plant tissues.

RESULTS

UV irradiation of (±)-ABA

For specific binding between ligand and receptor to occur, both must retain their native conformation. Thus, the stability of (±)-ABA was investigated upon irradiation at different lower irradiation boundaries for different periods of time. Figure 1 shows the effect on isomerization and photolysis of (±)-ABA as the lower irradiation boundary is raised by inserting cut-on filters. Both the rate of (±)-all *trans*-ABA formation and (±)-ABA photolysis was reduced as the cut-on value of the inserted filter was increased, as summarized in Table 2.

Photolysis of (±)-ABA was highly wavelength dependent, with only 8.7% remaining after irradiation for 10 min with the lower boundary set at its lowest value (no filter inserted), and as much as 70% if a WG345 filter was used. Without filter both (±)-ABA and (±)-all *trans*-ABA were lost, before an equimolar mixture was reached (Fig. 1A). Inserting a WG305 or WG320 filter reduced the rate of both processes (Fig. 1B), whereas insertion of a WG345 filter largely prevented isomerization without a clear effect on the total amount of (±)-ABA remaining (Fig. 1C, D, Table 2).

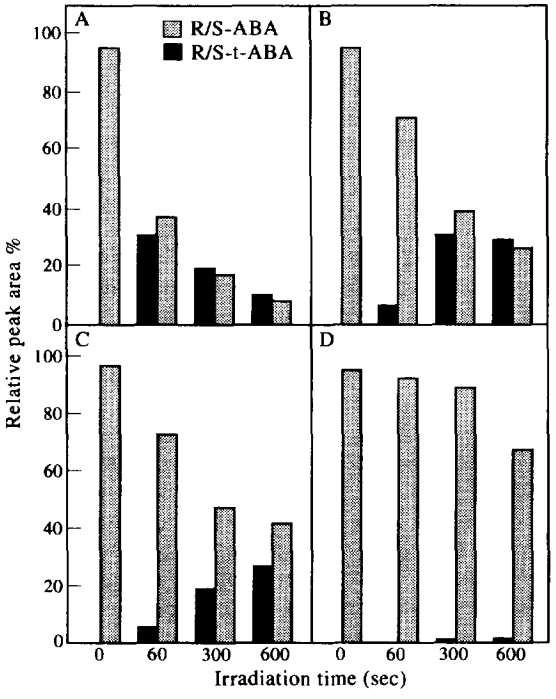

Fig. 1. Effect of UV irradiation on (±)-ABA in water using different cut-on filters. The samples were analysed by HPLC. A: no filter used; B: 305 nm filter; C: 320 nm filter and D: 345 nm filter. Mean and s.e. of two independent experiments.

Table 2. Effect of long pass filters on ABA photolysis and isomerization when exposed to continuous UV irradiation[a]

Time (s)	No filter			WG305			WG320			WG345		
	ABA	Ratio[b]	Sum[c]	ABA	Ratio	Sum	ABA	Ratio	Sum	ABA	Ratio	Sum
0	99.9	999.0	100.0	99.9	999.0	100.0	99.9	999.0	100.0	99.9	999.0	100.0
60	38.4	1.2	70.2	75.6	10.6	82.7	75.8	14.4	81.1	96.2	304.7	96.5
300	18.2	0.9	38.3	40.6	1.3	72.7	50.3	2.6	69.9	91.7	96.8	92.6
600	8.7	0.8	19.6	28.0	0.9	57.7	43.5	1.6	70.7	70.3	74.2	71.3

[a]Only HPLC peaks corresponding to (±)-ABA and (±)-all *trans*-ABA are taken into account. Data in percentages relative to ABA-peak.

[b]Ratio (±)-ABA to (±)-all *trans*-ABA.

[c]Total peak area of (±)-ABA and (±)-all *trans*-ABA.

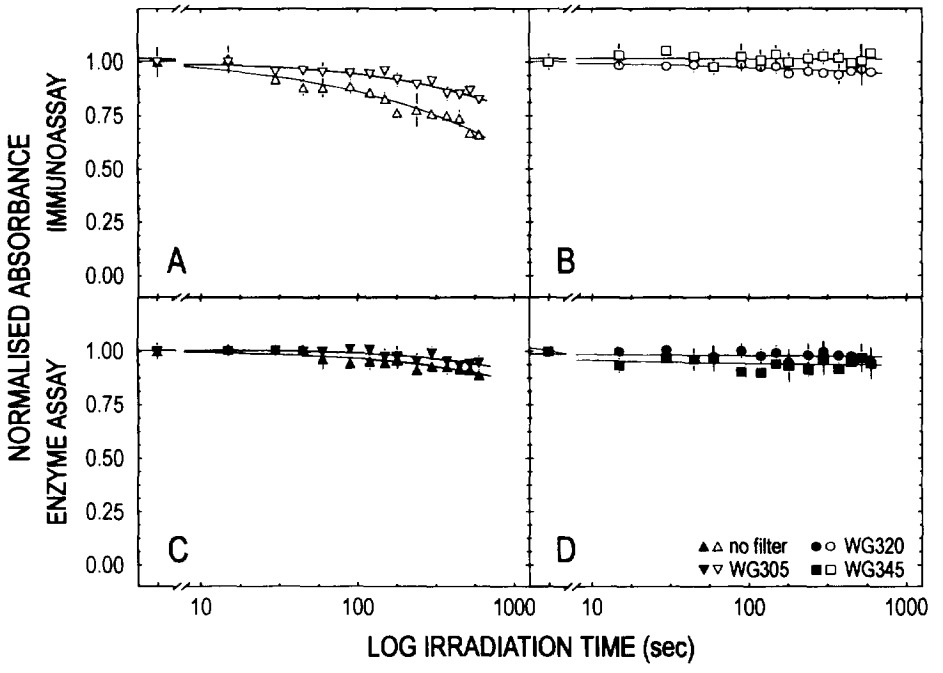

Fig. 2. Effect of UV irradiation using different cut-on filters on C_1-conjugated (±)-ABA (panels A and B) and enzymatic activity as measured by AP (panels C and D). Remaining ABA molecules were measured using (±)-ABA-C_1-AP on microtitre plates coated with goat anti-mouse and the anti-ABA antibody 3G4 (see Fig. 7: direct method). Mean and s.e. of two independent experiments in triplicate.

UV irradiation of conjugated (±)-ABA

It was hypothesized that (±)-ABA, when conjugated to protein, may be shielded from the isomerizing and photolysing effects of UV irradiation. Therefore, the stability of (±)-ABA conjugated to alkaline phosphatase (ABA-C_1-AP) was also analysed. This permitted both following of the fate of ABA and assessing the possibly damaging action of UV irradiation on AP enzymatic activity and structural integrity. Combined isomerization and photolysis of ABA were quantified by loss of binding of the irradiated ABA-C_1-AP to the specific anti-ABA antibody 3G4 (Fig. 2). Without a filter, 35% of immunologically detectable (±)-ABA, but only 10% of AP enzymatic activity, was lost upon irradiation for 10 min (Fig. 2A, C). In contrast, inserting a WG320 or WG345 filter to raise the lower irradiation boundary essentially prevented photolysis of (±)-ABA or loss of AP-activity (Fig. 2B, D).

Since the immunoassay for (±)-ABA (Fig. 2A, B) is dependent upon the activity of AP (see Fig. 7: direct method), the loss of (±)-ABA depicted is overestimated when AP activity is not fully maintained. Correcting for the loss of AP activity, approximately 79% of the (±)-ABA was still present after 10 min of irradiation without filters. This is substantially more than upon irradiation of free (±)-ABA under the same conditions. Thus, associa-

tion of ABA with a binding protein can be expected to have a stabilizing effect on the hormone molecule.

Protein stability under UV

Although AP enzymatic activity was relatively unaffected by UV irradiation, other proteins might be more susceptible. To study the effect of various wavelengths on protein conformation, mouse monoclonal anti-ABA antibodies 3G4 and Nan1 were subjected to irradiation and their binding properties evaluated in both direct and indirect assays. Any loss of structure would be evident as a loss of binding to goat anti-mouse antibodies and/or ABA conjugates.

Similarly to the enzymatic activity of AP, the binding activities of the antibodies to ABA-C_1-AP (Fig. 7: direct method) were reduced by about 30% after 10 min irradiation without a filter (Fig. 3A). In contrast to AP, the antibodies were not significantly affected when a WG305 filter was used (Fig. 3B). Raising the lower irradiation boundary further by inserting a WG320 or a WG345 filter prevented any loss of (±)-ABA-binding activity or recognition by goat anti-mouse antibodies (Fig. 3C, D). Analysis of binding of UV-irradiated anti-ABA antibodies to (±)-ABA-C_1-KLH (Keyhole Limper hemocyanine) (Fig. 7: indirect method) gave the same results (data not shown).

Photoaffinity cross-linking of anti-ABA antibodies to immobilized (±)-ABA

On UV irradiation only part of the ligand-binding protein complexes formed, is cross-linked. To assess photoaffinity cross-linking, non-covalently bound molecules have to be removed by washing, whereas the coating of the plates to which the cross-linked proteins are attached, must remain intact.

From a series of experiments with several types of washing buffer, it appeared that the protein coating could withstand the rather harsh treatments (acidic urea) necessary to remove non-cross-linked antibodies (data not shown). As shown in Fig. 4A, antibody binding was retained when either glycine–HCl buffer (pH 3.0) or phosphate buffered saline PBST was used. Even addition of up to 8 M urea did not affect the coating (Fig. 4A). Antibodies could not be removed by washing with PBST, but binding was completely disrupted under acidic conditions in the presence of urea (Fig. 4B). Addition of 100 μM (±)-ABA to the washing buffer prevented reassociation of anti-ABA antibody and coated (±)-ABA-C_1-KLH conjugate (data not shown). Thus, essentially complete removal of non-covalently bound antibodies was obtained by soaking the plates once for 10 min in 250 mM glycine–HCl (pH 3.0), 6 M urea. These conditions did not affect the coating.

Conditions for irradiation of the antibodies were varied so as to maximize cross-linking, while minimizing photolysis. As the lower irradiation boundary was raised protein photolysis was nearly eliminated, leaving photoinduced cross-linking (Fig. 5B–D). Raising the lower irradiation boundary beyond the wavelength necessary to excite the enone oxygen electrons resulted in a loss of cross-linking efficiency (Fig. 5D). Prolonging irradiation beyond 5 min had no effect on the efficiency of photoinduced cross-linking. Absorption to the microtitre plate,

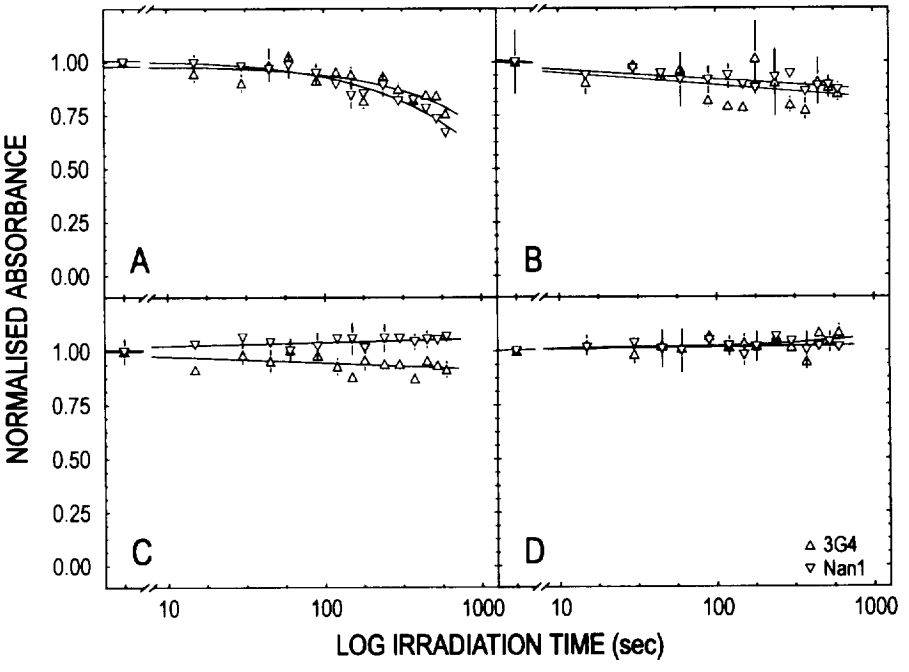

Fig. 3. Stability of monoclonal antibodies under UV irradiation using different cut-on filters. After irradiation samples were analysed in goat anti-mouse-coated microtitre plates. Remaining anti-ABA activity was measured with (±)-ABA-C_1-AP (see Fig. 7: direct method). Mean and s.e. of two independent experiments in triplicate.

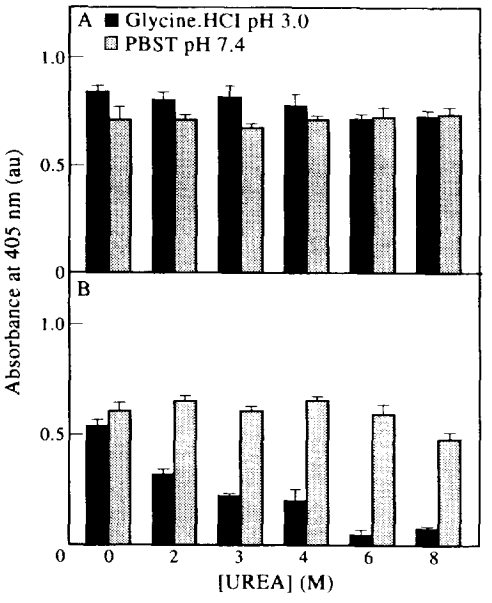

Fig. 4. Plates were washed with the indicated buffer before or after antibody addition. In A, coated plates were washed prior to antibody addition. In B, the affinity washing was performed after antibody addition. Plates were then analysed using goat anti-mouse antibodies conjugated to AP (see Fig. 7: indirect method). The optical density is a measure for the remaining anti-ABA antibodies. Mean and s.e. of two independent experiments in triplicate.

as well as cross-linking of solute proteins to the coating protein, were estimated similarly using carrier protein coatings without conjugated (±)-ABA (data not shown). Such non-specific binding was found to be substantial, especially when using the mouse pre-immune serum. Corrections were made as described in the Experimental.

Since the anti-ABA antibodies 3G4 and Nan1 differ in their affinity towards ABA, differences in UV-induced cross-linking efficiency were expected. As is clear from Fig. 5B, Nan1 was cross-linked substantially more than 3G4 under optimal irradiation conditions. The non-specific antibodies in mouse pre-immune serum are barely cross-linked to the (±)-ABA-C_1-KLH conjugate, whereas the anti-ABA antibody Nan2 (C_4-conjugated ABA specific) was only slightly better cross-linked (Fig. 5). These results demonstrate that cross-linking faithfully reflects cognate binding activity.

DISCUSSION

The basic requirements for successful photoaffinity labelling are summarized in Table 1. In the present study, these requirements were extended to define conditions necessary to cross-link ABA specifically to ABA-binding protein(s). Because of its natural photosensitivity its use as a photoaffinity ligand offers a great advantage over synthetic analogues. ABA contains two distinct chromophores that contribute to its UV spectrum: the enone

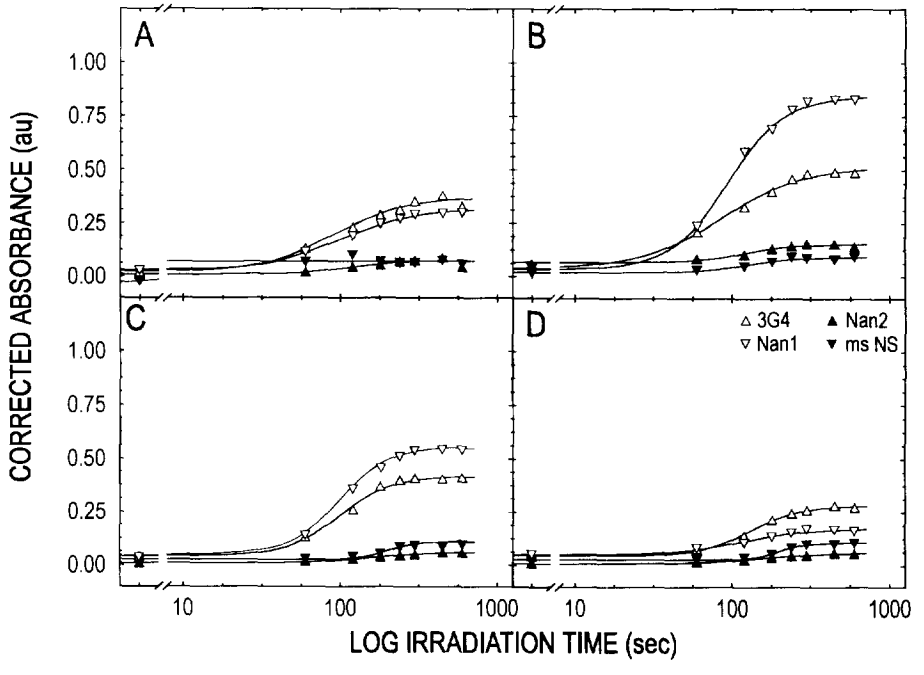

Fig. 5. Cross-linking of mouse monoclonal anti-ABA (C_1-conjugated) antibodies 3G4 and Nan1, mouse monoclonal anti-ABA (C_4-conjugated) antibody Nan2 and mouse pre-immune serum to (±)-ABA-C_1-KLH-coated wells of microtitre strips. The data are corrected for a specific cross-linking of the antibodies to unconjugated KLH and absorption to well walls. Cut-on filters used: A: no filter; B: 305 nm; C: 320 nm; D: 345 nm. Mean and s.e. of two independent experiments in duplicate.

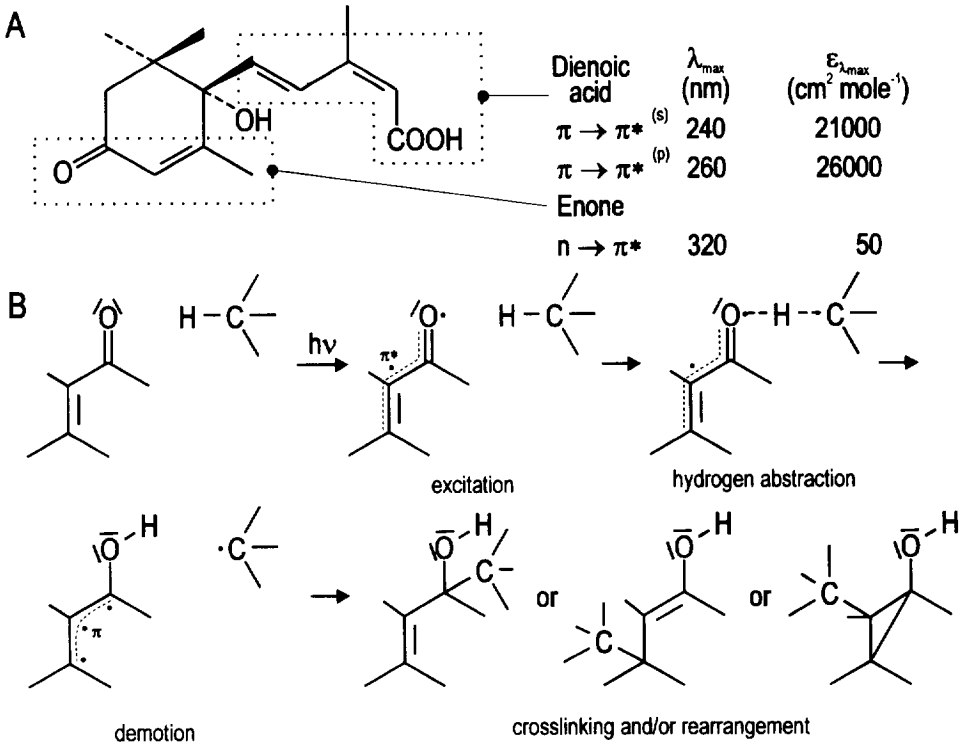

Fig. 6. Absorption maxima of the ABA chromophores as measured in acidic (0.005 N H_2SO_4) MeOH (A). The absorption data were taken from [27] ($\pi \rightarrow \pi^*$ transitions) or measured in acidic MeOH ($n \rightarrow \pi^*$ transitions). B shows a general scheme of enone insertion in a C–H bond after UV-induced $n \rightarrow \pi^*$ excitation [6, 23, 24]. Cross-linking is initiated by *inter*molecular hydrogen abstraction.

moiety in the ring and the doubly conjugated carboxylic acid moiety in the side chain (Fig. 6A). Both chromophores can be excited in a $\pi \rightarrow \pi^*$ transition, but only the enone gives rise to the (n, π^*) states required for photoinduced cross-linking [6, 9].

Cross-linking can be thought of as an insertion of the photosensitive ligand into a bond (usually C–H) of the target protein (Fig. 6B) [10]. The cross-linking efficiency depends on the competition between the insertion (initiated by *inter*molecular hydrogen abstraction) and skeletal rearrangements (initiated by *intra*molecular hydrogen abstractions) [6, 18, 19]. This competition is influenced by the environment of the enone at the onset of excitation. If there is a suitably oriented protein hydrogen atom in the vicinity of the activated enone, *inter*molecular abstraction is likely to occur (Fig. 6B) [6, 20].

Only a few reports describing the effects of UV irradiation on the structural integrity of ABA have been published (e.g. [21, 22]). Such effects can, however, be predicted from data obtained for other enones and polymers [9, 23–25]. Three types of reactions are important in ABA photoaffinity labelling: isomerization (involving the side-chain chromophore), photolysis (involving both side-chain and enone chromophore) and hydrogen abstraction (involving the enone chromophore). Both isomerization and photolysis must be reduced as much as possible, while retaining hydrogen abstraction. This requires the lower irradiation boundary to be increased such that $\pi \rightarrow \pi^*$ transitions are virtually absent, leaving the $n \rightarrow \pi^*$ transitions (Fig. 6A). The molar extinction coefficient can be thought of as a measure of the efficiency of photon capture. Due to the difference in the molar extinction coefficient [$\varepsilon_{\lambda_{max}}(\pi \rightarrow \pi^*)$: 26 000 cm^2 $mole^{-1}$ vs $\varepsilon_{\lambda_{max}}(n \rightarrow \pi^*)$: 50 cm^2 $mole^{-1}$] the lower boundary must be close to λ_{max} for the $n \rightarrow \pi^*$ transition.

In the unconjugated ABA molecule both ring and side-chain are fully exposed to UV irradiation. When no filter is introduced in the UV beam, both photolysis and isomerization occur simultaneously (Fig. 1A). Increasing the lower irradiation boundary gradually filters out the wavelengths responsible for isomerization (around 260 nm) (Fig. 1B, C). As the boundary exceeds 318 nm, the $n \rightarrow \pi^*$ transitions are, likewise, strongly reduced, resulting in a near cessation of photolysis (Fig. 1D).

Plancher [22] irradiated ABA using a 254 nm UV source. This wavelength induces only the $\pi \rightarrow \pi^*$ transitions of both enone and side-chain chromophores. Apart from ABA and all *trans*-ABA, three minor products, supposedly the 4-*cis*-isomers and ABA-1′,4′-peroxide, were isolated. Irradiation resulted in near-equimolar mixtures of ABA and all *trans*-ABA, while photolysis reduced the total amount of ABA. Increased photolysis when the irradiating wavelength neared 310 nm, was observed by Brabham and Biggs [21]. By using HPLC analysis, we likewise found three minor products in addition to the all *trans*-ABA peak (data not shown), as well

as loss of total ABA. These results demonstrate the importance of selecting an optimal wavelength for ABA cross-linking studies.

Conjugating ABA to a protein through its side-chain induces a red shift in the λ_{max} of this chromophore and shields it from UV irradiation. On the other hand, susceptibility of the protein towards UV photolysis might be enhanced by intersystem crossings of excited ABA side-chain to aromatic or sulphur-containing amino acids [5, 8, 11]. However, conjugation of ABA to proteins appeared to stabilize it towards photolysis and possibly isomerization. Loss of ABA was not as severe as the loss of unconjugated ABA under the same conditions (Figs 1A, B and 2A). Protein photolysis also occurred (Figs 2C and 3A, B), but as the lower boundary was raised above 290 nm ($\tau < 0.01$) photolysis of proteins was no longer detectable.

Conjugation of ABA to protein may sterically hinder its association with, and hence its affinity towards, a binding protein. Only proteins binding ABA at its cognate binding site at the moment of irradiation can be specifically cross-linked. The extent of cross-linking is determined by the reactant's orientation and environment [5, 8, 19]. Other proteins might become cross-linked, if the ABA diradical intermediates have a relatively long lifetime, resulting in pseudo-affinity labelling or non-specific attachment [7, 12–14]. Non-specific cross-linking also occurs if solute proteins generate photoactivated amino acid residues, notably the aromatic residues, that are able to cross-link this protein to the coating matrix [5, 8]. We demonstrated, that all non-covalently bound proteins remaining attached to the coating as the irradiated solution is discarded, can be removed by washing with acidic urea (Fig. 4).

By conjugating ABA through either the side-chain or the ring, discrimination between putative ABA-binding proteins is possible, as demonstrated in Fig. 5. Those proteins that specifically recognize the ring structure are bound by C_1-immobilized ABA, whereas those recognizing the side-chain can not bind. Anti-ABA antibodies raised against C_1-conjugated ABA (3G4 and Nan1) were specifically cross-linked to the ABA-C_1-KLH conjugate, whereas the anti-ABA antibody Nan2, raised against C_4-conjugated ABA, was hardly so. Moreover, the influence of the affinity towards the ring structure on the cross-linking efficiency is exemplified by Nan1 and 3G4. The displacement of Nan1 by an increasing amount of ABA from ABA-C_1-KLH-coated microtitre plates required a two log units higher concentration of free ABA than 3G4. Since binding was specific, this indicates a much stronger affinity for conjugated ABA on the part of Nan1, and consequently a higher cross-linking efficiency (Fig. 5B).

From the optimization of the UV-cross-linking conditions, it can be concluded that C_1-conjugated ABA is an excellent photoaffinity label, provided the lower boundary of the irradiating UV light is above 290 nm. Maximal cross-linking is achieved within 5 min, minimizing UV-induced photolysis or activity loss of proteins. Conjugation of ABA not only stabilizes this ligand, but also allows its immobilization as a coating on microtitre plates, facilitating the separation of bound or cross-linked and non-attached binding proteins. The method should be applicable to the identification and analysis of ABA-binding proteins in plant extracts.

EXPERIMENTAL

Antibodies. The mouse anti-ABA monoclonal antibody 3G4 [26] and the ABA-C_1-KLH conjugate were obtained from Dr C. Vonk (DLO-CABO, Wageningen, The Netherlands). 3G4 was raised against pig thyroglobulin C_1-conjugated ABA. The mouse anti-ABA monoclonal antibodies Nan1 and Nan2 were a gift from Prof. X. Zhou (Nanjing University, Peoples Republic of China). Nan1 was raised against (±)-ABA-C_1-BSA, whereas Nan2 was raised against (±)-ABA-C_4^1-BSA. These antibodies were chromatographically purified and stored, lyophilized, in the presence of BSA. Nan1 was diluted to give the same signal as 3G4 in an indirect ABA-enzyme immunoassay standard curve. Nan2 was used at arbitrary dilution (atmost at the dilution used for Nan1).

Synthesis of ABA-C_1-AP. ABA was converted to its *N*-hydroxysuccinimide (NHS) ester by adding 15.6 mg (75 μmol) dicyclohexylcarbodiimide to a stirred soln of 2.6 mg (10 μmol) ABA and 1.2 mg (11 μmol) NHS in 1 ml dioxan. The reaction was initiated by the addition of 10 μl 0.1 M HCl in water and allowed to proceed overnight at room temp. Then 10 μl 1 M HCl was added. After another hr the pptd dicyclohexylurea was filtered off using a Millipore AP25 filter. Conversion was checked by HPLC using a RP C_{18}-column eluted with MeOH–H_2O (1:1), containing 0.01% HOAc.

Dioxan was evapd in a fume hood under a flow of air. The residue was dissolved in 100 μl DMF and added to 1 ml 50 mM Na-P_i buffer (pH 8.5), containing 1 mg AP (EC 3.1.3.1; 33.4 μkat mg^{-1}). Conjugation was allowed to proceed overnight at 4° under stirring.

The ABA-C_1-AP was concentrated in a Microcon-100 (Amicon) and washed twice with Tri-TES buffered saline (TTBST) containing 0.5% (w/v) BSA. The final retentate was recovered, diluted to 1 mg ml^{-1} with washing buffer and stored at 4°. Enzyme activity was tested by adding 10 μl of a dilution series in TTBST to 200 μl 1 mg ml^{-1} *p*-minophenyl phosphate (*p*NPP) in coating buffer. The conjugate was also tested in a direct assay (Fig. 7) using free ABA as competitor.

Immunoassays. Flat-bottomed microtitre plates, 8-well strips, seals and lids were obtained from Costar Nucleopore. During the incubation periods plates or strips were always sealed, covered and placed on a tightly fitting piece of Al before wrapping in Al foil. The sealing prevented solvent evapn, whereas the 3 mm thick metal slab ensured an evenly distributed incubation temp. Unless stated otherwise, incubations were typically 3 hr at 35° and plates were washed ×6 with PBST between incubations. Enzymatic colour development was stopped by adding 50 μl 5 M KOH to each well when an absorbance above 1.2 was reached. Ten min later the plates were

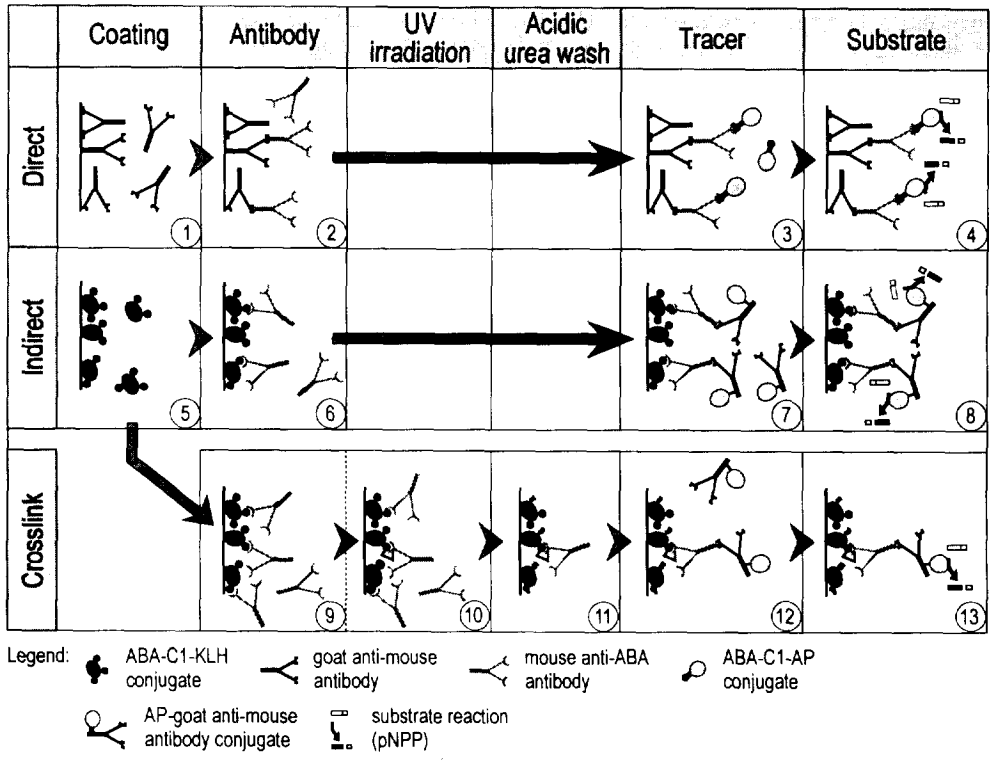

Fig. 7. Diagram of the enzyme immunoassay procedures used in this study. Each box represents a treatment followed by washing, while each arrow indicates a transition from one incubation to the next. 1 and 5: coating of strips with goat anti-mouse antibodies or (±)-ABA-C_1-KLH, respectively; 2, 6 and 9: addition of mouse anti-ABA antibodies; 3, 7 and 12: addition of (±)-ABA-C_1-conjugated or goat anti-mouse-conjugated AP; 4, 8 and 13: enzymatic assay using pNPP as substrate; 10: UV irradiation of samples; 11: removal of non-covalently bound antibodies by washing. For further explanation, see Experimental.

read at 405 nm on a Merck MIOS-reader (Dynatech 7000).

Plates or strips were coated with 200 μl well^{-1} of protein (10 μg ml^{-1}) or goat anti-mouse antibody (1 μg ml^{-1}) soln in coating buffer (34.8 mM $NaHCO_3$, 16.0 mM Na_2CO_3 (pH 9.6), 6.5 mM NaN_3, 0.5 mM $MgCl_2$). Plates were incubated for at least 24 hr at 4° and washed ×2 with H_2O and 3× with PBST (8.1 mM Na_2HPO_4, 1.5 mM KH_2PO_4 (pH 7.3), 137 mM NaCl, 2.7 mM KCl, 6.5 mM NaN_3, 0.05% (v/v) Tween-20) using a Merck washer (Dynatech MR 7000). Thereupon, either of three types of assay procedures were followed, as outlined in Fig. 7.

1. *Direct assay*: Goat anti-mouse-coated plates were used (1). A soln of mouse anti-ABA antibodies in TTBST (as PBST, but with 10 mM Tris–HCl and 10 mM TES (pH 7.4) instead of the phosphate salts) was added (2). After incubation the plates were blocked with 1% (w/v) BSA in 50 mM Na-P_i buffer (pH 8.5) for 1 hr at room temp. Binding of ABA protein conjugate was then analysed with 200 μl well^{-1} (±)-ABA-C_1-AP (100 ng ml^{-1}) in TTBST containing 0.5% (w/v) BSA (3), followed by pNPP (200 μl well^{-1}, 1 mg ml^{-1}) in coating buffer (4).

2. *Indirect assay*: Plates were coated with (±)-ABA-C_1-KLH (5). To each well, 200 μl of anti-ABA antibodies 3G4 or Nan1 in TTBST was added (6). The amount of mouse antibodies retained in the wells, was subsequently assayed using goat anti-mouse-AP conjugate in TTBST containing 0.5% (w/v) BSA (200 μl well^{-1}) (7), followed by pNPP in coating buffer (8).

3. *Photoaffinity labelling*: This procedure was adapted from the indirect assay, using (±)-ABA-C_1-KLH-coated strips. After incubation with mouse antibodies (9), wells were irradiated in order to cross-link the antibody to (±)-ABA-C_1-KLH (10). To remove non-covalently bound antibodies after irradiation, strips were soaked ×3 with 250 μl well^{-1} of 250 mM glycine–HCl (pH 3.0) containing 6 M urea for 10 min at ambient temp. (11). After the third soaking strips were washed with H_2O (×2), followed by PBST (×3). The strips were then treated as described for the indirect assay (12, 13).

Light source and sample irradiation. There is no consensus about the equipment to be used in photoaffinity labelling (see refs cited in [5] and [7]). UV sources vary from magnesium flash bulbs to 1 kW Xe(Hg) pressure lamps. Samples have been irradiated discontinuously in multiple, short pulses or continuously for 1–10 min, at distances ranging from 1–30 cm. To study ABA cross-linking, a UV source similar to the one used by Hornberg and Weiler [2] was adapted to optimize irradiation conditions.

An Oriel UV source equipped with a HBO 500 W/2 Hg arc lamp (Ushio) was used in all cross-linking experiments. An optical system was fitted to the lamp house to

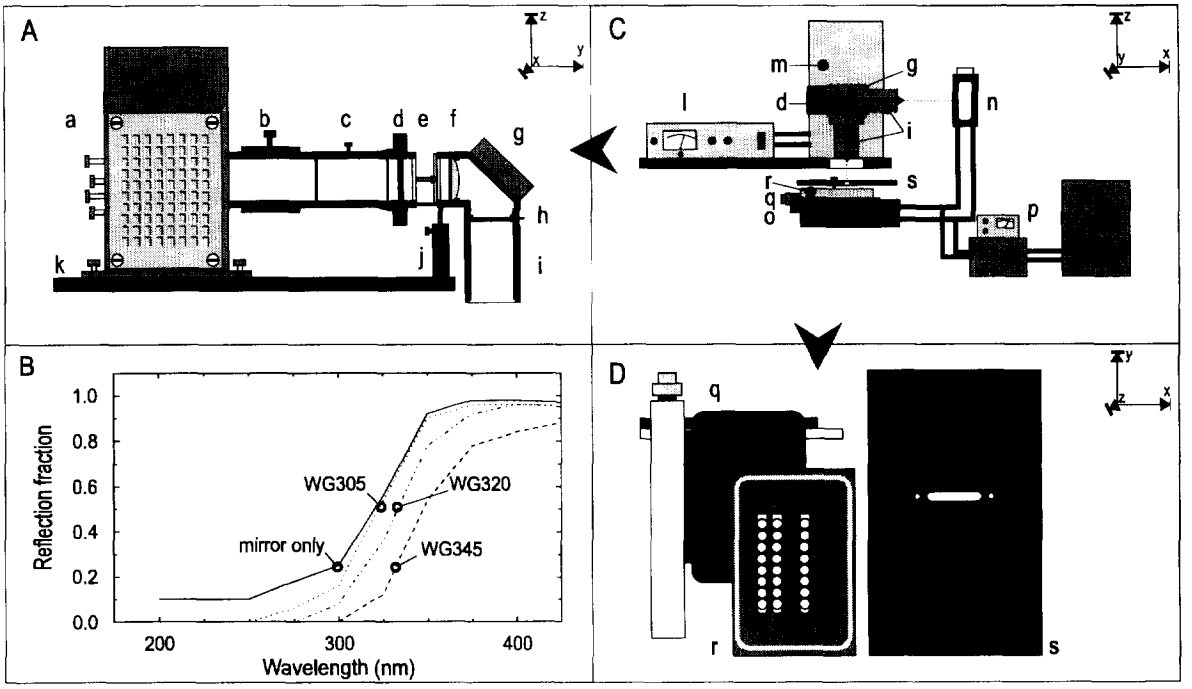

Fig. 8. Schematic diagram of the UV equipment used to cross-link ABA to proteins. A: side view of the optical system: a: lamp house; b: lineator; c: water filter; d: shutter; e: filter holder; f: condensing lens; g: dichroic mirror; h: diaphragm; i: tube; j: supporting rod; k: ground plate. The effect of cut-on filter insertion on the lower spectral boundary of the dichroic mirror is shown in B. C shows the front view of the complete set-up (vertical and horizontal orientation is indicated by the knicked arrow): l: power supply; m: lamp house and optical system (details shown in A); n: cuvette holder; o: microtitre strip holder (details shown in D); p: cooling unit. D is a top view of the assembly for irradiating microtitre strips: q: plate attached to cross-table on box; r: strip holder showing strips in slots and positioning holes; s: PVC cover plate with slot and positioning pins. The axes indicate the plane at which the diagram is positioned.

obtain a versatile set-up (details given in Fig. 8A). The whole set-up was placed in a rack, covered with UV-impermeable perspex. Sample temp. was maintained at about 0° using a thermostat bath coupled to a cooling unit.

By turning the dichroic mirror, samples in either cuvettes or microtitre strips could be irradiated (Fig. 8C). Quartz cuvettes were placed in a cooled, windowed jacket. A mirror in the opposite wall of the jacket reflected the incoming beam back into the test soln. Strips were cooled by inserting them into slots in an Al block, fitting tightly on a cross-table (details in Fig. 8D). This cross-table was fitted to a cooled container. A PVC plate was placed directly above the plates to prevent irradiation of adjacent wells. A slit in the plate exposed a row of four wells to the light beam. Exact positioning was obtained by manipulation of the cross-table and pins passing through the plate into the Al block.

The dichroic mirror was used to create a UV band with a lower boundary at 260 nm and an upper one at 530 nm (reflection at or beyond boundaries, less than 10%). Long pass, cut-on filters (WG*xxx*, where *xxx* indicates the wavelength) were obtained from Schott. These filters were used to selectively increase the lower boundary, i.e. reduce irradiance at the lower wavelengths (Fig. 8B). All filters were 2 mm thick and had an internal transmittance (τ_i) of 0.81 at the indicated wavelength. The transmittance (τ) and spectral irradiance (E_e) at other wavelengths were calculated using the physical properties given by the manufacturer (Table 3).

Table 3. Transmittance and spectral irradiance of the UV beam at different wavelengths using different long pass, cut-on filters using a HBO 500 W/2 Hg arc lamp as source (data collected from Schott catalogue 3531/4d and Oriel Euro catalogue vol. II)

λ	300 nm		350 nm		400 nm	
Filter	τ[a]	E_e[b]	τ	E_e	τ	E_e
None	–	1.25	—	0.97	—	4.82
WG305	0.56	0.70	0.92	0.89	0.92	4.43
WG320	0.04	0.05	0.87	0.84	0.90	4.34
WG345	$2 \cdot 10^{-9}$	$3 \cdot 10^{-9}$	0.75	0.73	0.83	4.00

[a]Transmittance for 2 mm thick filters calculated according to $\tau = P \cdot \tau_i^2$ (P, τ_i obtained from Schott catalogue).

[b]Estimated spectral irradiance in $mW\,cm^{-2}\,nm^{-1}$ of UV-beam at given wavelength corrected for reflection values of optical system components as given by manufacturers.

Sample irradiation. Proteins (3G4, NanI and AP) and conjugated ABA (as (±)-ABA-C_1-AP) were irradiated in

TTBST either in quartz cuvettes or in microtitre strips. Photo-oxidation was prevented by NaN_3, present in the buffers [5]. Samples (200 μl) were withdrawn from the cuvettes at indicated time intervals, placed on ice and analysed. Wells from microtitre strips were individually sampled. Anti-ABA antibodies were analysed using the direct assay. To follow the fate of ABA when conjugated to protein, samples (50 μl 200 ng ml^{-1}) were made up to 200 μl well^{-1} with TTBST containing 0.5% (w/v) BSA, and assayed for binding to 3G4. AP activity was checked by adding 10 μl diluted (±)-ABA-C_1-AP samples to 200 μl pNPP in coating buffer.

Abscisic acid analysis by HPLC. Free (±)-ABA was irradiated at 100 μM in H_2O. Samples (200 μl) were taken at the indicated times and placed on ice. Then, 100 μl of each sample was subjected to HPLC (Chrompack): RP C_{18} prep. column (Chrompack μBond; 250 × 10 mm) eluted with a linear gradient of 10 to 80% MeOH in H_2O containing 0.01% HOAc. The eluent was monitored at 267 nm. All samples were analysed relative to the peak area of a 100 μl 100 μM (±)-ABA standard. The R_ts of (±)-all *trans*-ABA and (±)-ABA were determined by injection of the pure isomers and used as calibration.

UV-induced cross-linking. Strips, coated with (±)-ABA-C_1-KLH or unmodified KLH, were incubated with mouse antibodies. The (±)-ABA-C_1-KLH-coated strips were placed in the middle slots of the block, flanked by KLH-coated strips in the outer slots. Four wells were irradiated simultaneously (one of each strip) for the indicated time. The power supply was set at 450 W. Filters were inserted into the beam to vary the lower boundary of the UV band. Irradiated strips were placed on ice prior to analysis as described under photoaffinity labelling. The KLH-coated strips were used as controls to measure absorption and non-specific cross-linking of the mouse antibodies. These values were substracted from the (±)-ABA-C_1-KLH measurements to obtain the photoaffinity cross-linking curve.

Acknowledgements—The authors wish to express their gratitude to the technical staff of the Department of Plant Physiology who helped to build the UV set-up (Mr R. van der Laan), made the positioning table (Mr B. van der Swaluw) and manufactured the strip container (Mr J. van Kreel). A special word of thanks is directed to Miss Chr. Meyer, who introduced one of us (M.H.M.C.) to photoaffinity labelling during his stay at the Lehrstuhl für Biologie of the Ruhr Universität, Bochum (F.R.G.), and to his host Prof. Dr E. W. Weiler.

REFERENCES

1. Weselake, R. J. and Jain, J. C. (1992) *Physiol. Plant* **84**, 301.
2. Hornberg, C. and Weiler, E. W. (1984) *Nature* **310**, 321.
3. Napier, R. M. and Venis, M. A. (1990) *J. Plant Growth Regul.* **9**, 113.
4. Willows, R. D. and Milborrow, B. V. (1993) *Phytochemistry* **32**, 869.
5. Bayley, H. (1983) in *Photogenerated Reagents in Biology and Molecular Biology*, 2nd edn. Elsevier Scientific Publishers, Amsterdam.
6. Dormán, G. and Prestwich, G. D. (1994) *Biochemistry* **33**, 5661.
7. Gronemeyer, H. (1985) *TIBS* **10**, 264.
8. Goeldner, M. P., Hirth, C. G., Kieffer, B. and Ourisson, G. (1982) *TIBS* **7**, 310.
9. Turro, N. J. (1978) in *Modern Molecular Photochemistry*. Benjamin/Cummings, Menlo Park.
10. Martyr, R. J. and Benisek, W. F. (1973) *Biochemistry* **12**, 2172.
11. Galardy, R. E., Craigh, L. C., Jamison, J. D. and Printz, M. P. (1974) *J. Biol. Chem.* **249**, 3510.
12. Katzenellenbogen, J. A., Johnson, H. J. J., Carlson, K. E. and Myers, H. N. (1974) *Biochemistry* **13**, 2986.
13. Payne, D. W., Katzenellenbogen, J. A. and Carlson, K. E. (1980) *J. Biol. Chem.* **255**, 10359.
14. Standring, D. N. and Knowles, J. R. (1980) *Biochemistry* **19**, 2811.
15. Dure, L. S., IV, Schrader, W. T. and O'Malley, B. W. (1980) *Nature* **283**, 784.
16. Venis, M. A. (1984) *Planta* **162**, 502.
17. Weiler, E. W. (1980) *Planta* **148**, 262.
18. Turro, N. J., Dalton, C., Dawes, K., Farrington, G., Hautala, R., Morton, D., Niemczyk, M. and Schors, N. (1972) *Acc. Chem. Res.* **5**, 92.
19. Turro, N. J. and Ramamurthy, V. (1977) *Mol. Photochem.* **8**, 239.
20. Dauben, W. G., Salem, L. and Turro, N. J. (1975) *Acc. Chem. Res.* **8**, 41.
21. Brabham, D. E. and Biggs, R. H. (1981) *Photochem. Photobiol.* **34**, 33.
22. Plancher, B. (1979) *Gartenbauwissenschaften* **44**, 184.
23. Schaffner, K. (1966) *Adv. Photochemistry* **4**, 81.
24. Wagner, P. J. and Hammond, G. S. (1968) *Adv. Photochemistry* **5**, 21.
25. Woodward, R. B. (1941) *J. Am. Chem. Soc.* **63**, 1123.
26. Boonekamp, P. M., Pomp, H., Davelaar, E. and Voule, C. R. (1990) in *Monoclonal Antibodies in Agriculture* (Schots, A., ed.), p. 37. PUDOC, Wageningen, The Netherlands.
27. Dörffling, K. and Tietz, D. (1983) in *Abscisic Acid* (Addicot, F. T., ed.), p. 27. Preager Publishers, New York.
28. Beale, M. H., Hooley, R., Smith, S. J. and Walker, R. P. (1992) *Phytochemistry* **31**, 1459.